ISBN: 978-3-95450-231-8 ISSN: 2673-5490 doi: 10.18429/JACoW-IPAC2023-WEPL018

ANALYSIS OF THE DIAMOND-II BOOSTER DIPOLE MAGNETS

I.P.S. Martin*, B. Nicholson, Diamond Light Source, Oxfordshire, UK

Abstract

As part of the Diamond-II upgrade project, the booster synchrotron is due to be replaced with a low-emittance solution that enables efficient injection into the Diamond-II storage ring. The new booster lattice uses cells of combined-function gradient bends that integrate dipole, quadrupole and sextupole components into single magnets, alternating between focussing and defocussing bends. Accurate modelling of these magnets in particle tracking codes is vital to ensure the beam dynamics is accurately simulated during the entire ramp. In this paper we report on the methods used to correctly model the Booster-II dipole magnets and summarise the impact on lattice performance.

INTRODUCTION

As part of the Diamond-II upgrade project [1], the existing booster synchrotron will be replaced with a new low-emittance ring [2, 3]. This will ensure high injection efficiency into the new storage ring, both by lowering the electron beam emittance and by reducing the bunch length at extraction. The extraction energy has been increased from 3 to 3.5 GeV to match the new storage ring energy, and the booster impedance has been kept low to maximise the charge per shot and to preserve beam quality at extraction.

The new booster contains three types of normal and combined-function dipoles, the design parameters for which are summarised in Table 1. During the lattice design studies the magnets were assumed to be idealised hard-edge sector-bend dipoles with parallel entrance and exit faces. In reality however, these magnets have extended fringe fields, and each of the multipole components have different magnetic lengths which can vary during the ramp due to remanent fields and saturation effects. In addition, unwanted multipole components can exist, particularly in the fringe region.

In this paper we present an analysis of the combined-function dipole magnet fields extracted from the OPERA [4] models. The methods used to incorporate the realistic magnet fields in the AT2 [5] tracking code model will be described, and the expected lattice parameters during the ramp will be shown.

Table 1: Booster Dipole Design Parameters

Parameter	Normal	Focussing	Defocussing
Name	BB	BF	BD
Number	4	36	38
Length (m)	1.25	1.30	1.30
Int. B (Tm)	1.19	0.55	1.28
Int. G (T)	0.0	14.5	-10.7
Int. S (T/m)	0.0	46.9	-57.2

* ian.martin@diamond.ac.uk

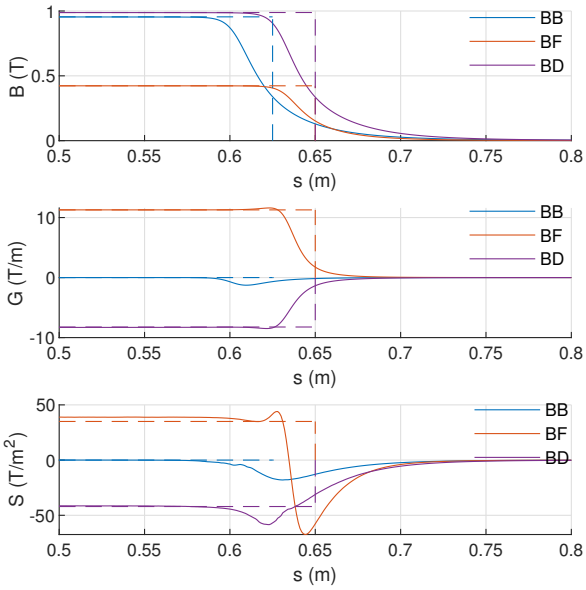

Figure 1: Dipole (top), quadrupole (middle) and sextupole (bottom) field components at 3.5 GeV as a function of distance from the magnet centres. Dashed lines show the design values for reference.

MAGNETIC FIELD ANALYSIS

A plot showing the magnetic field components as a function of distance through the magnets can be seen in Fig. 1. These plots highlight the significant deviation of the actual magnetic fields from the ideal hard-edge equivalent. For the BB dipoles, finite quadrupole and sextupole components can be seen in the fringe region. For the BF and BD dipoles, the bulk quadrupole and sextupole components had to be offset once to recover the correct integrated design values and a second time to reach the desired betatron tune values and nominal chromaticity when placed in the lattice.

Figure 2 shows how the effective lengths for the BD magnet multipole components vary during the ramp, where the effective lengths are defined as:

$$L_B = \frac{1}{B(0)} \int_{-\infty}^{\infty} B(s)\, ds$$
$$L_G = \frac{1}{G(0)} \int_{-\infty}^{\infty} G(s)\, ds \qquad (1)$$
$$L_S = \frac{1}{S(0)} \int_{-\infty}^{\infty} S(s)\, ds$$

The magnet design achieves close to the desired magnetic length for the dipole component only, with the quadrupole component shorter than the ideal magnet and the sextupole component significantly longer. Both the quadrupole and sextupole effective lengths deviate further from the desired values as the magnet starts to saturate.

ISBN: 978-3-95450-231-8 ISSN: 2673-5490 doi: 10.18429/JACoW-IPAC2023-WEPL018

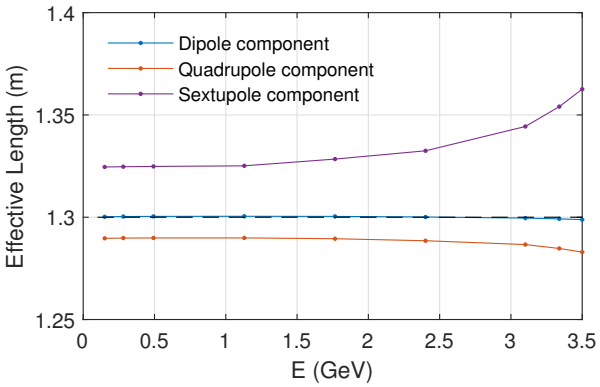

Figure 2: Effective dipole, quadrupole and sextupole lengths as a function of beam energy for the BD dipoles.

The integrated quadrupole and sextupole components for the BF and BD magnets are also found to vary during the ramp. These are shown in Fig. 3. As with the effective lengths, the strongest variation occurs as the magnets begin to saturate towards the extraction energy.

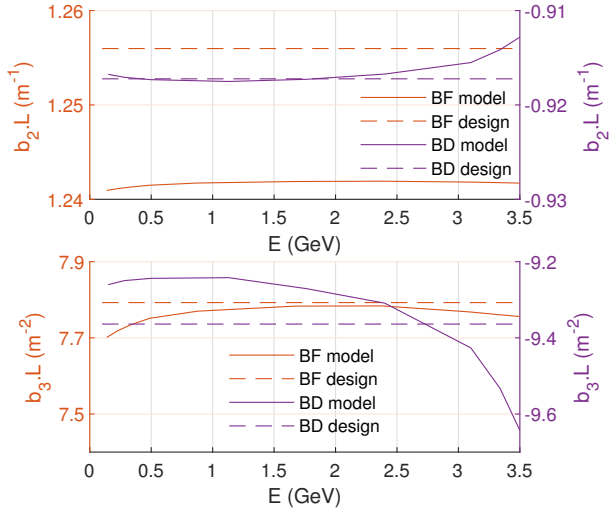

Figure 3: Integrated field values for the quadrupole (top) and sextupole (bottom) components as a function of beam energy for the BF and BD dipoles.

MAGNET MODELLING

To investigate how the observed field variations during the ramp are likely to impact the lattice performance, two methods of inserting the field data into the AT2 model have been studied. The first method is to insert the OPERA field data directly by splitting each magnet into 1 mm long segments, with each slice consisting of a sector bend element with multipole components up to 8th order set according to the local OPERA field data. This method is assumed to provide an accurate representation for the real magnets. However, the resulting tracking times are prohibitively long for the majority of studies.

As an alternative, a similar fitting method to that used in [6] was used to construct 'effective' hard-edge models. The method can be summarised as follows:

1. Build a simple transfer line consisting of [drift, thin lens, dipole, thin lens, drift], where the dipole length is equal to the original ideal magnet and the adjacent drifts are set to give the same total length as the sliced full-field data.

2. Build a grid of particles within the range x and y between ±8 mm, x' and y' between ±3 mrad and $\Delta p/p$ between ±3%.

3. Track the distribution through the sliced model to obtain a reference set of coordinates at the exit of the magnet.

4. Track through the effective hard-edge model, varying the bulk magnet and thin lens field components to minimise the difference between the final coordinates and those obtained from the sliced model.

Effective hard-edge dipole models were constructed in this way for a range of beam energies between 100 MeV (injection) to 3.5 GeV (extraction). In each case, the effective dipole models were found to accurately reproduce the betatron tune and chromaticity values calculated using the sliced magnet models as well as the beta-functions and dispersion. As a final check, on and off-momentum dynamic aperture and frequency maps were calculated using both dipole modelling methods with good agreement again found in the final results. A comparison of the on-momentum dynamic apertures is shown in Fig. 4. By using the effective hard-edge dipole approximation, the calculation time for the dynamic aperture was reduced from 33.5 h to 200 s.

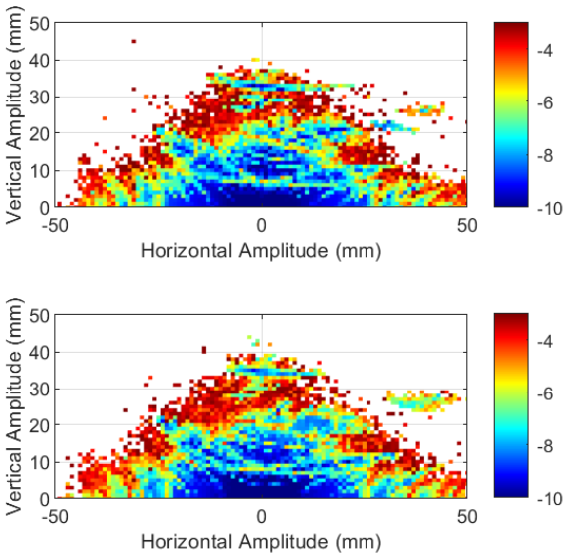

Figure 4: Comparison between dynamic apertures calculated using a sliced dipole model (top) and an effective hard-edge dipole approximation (bottom).

ISBN: 978-3-95450-231-8 ISSN: 2673-5490 doi: 10.18429/JACoW-IPAC2023-WEPL018

IMPACT ON LATTICE PARAMETERS

Having constructed practical models for the booster dipoles for use in tracking codes, these were then used to determine the impact on lattice and beam parameters. Shown in Fig. 5 are the resulting betatron tunes and chromaticity as a function of beam energy. The tunes are found to cross several potentially dangerous resonances during the ramp, including the $3Q_y$ skew sextupole resonance and $Q_x = Q_y$ coupling resonance. Chromaticity was found to be above target during the ramp, with a large increase in vertical chromaticity towards extraction. These effects are consistent with the observed variation in integrated quadrupole and sextupole field components discussed previouly.

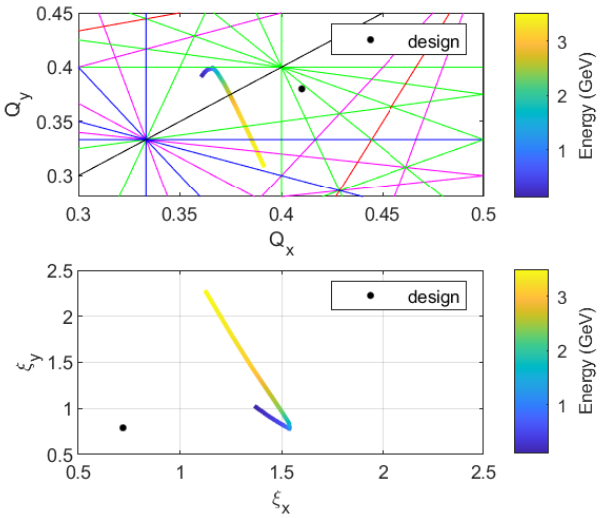

Figure 5: Betatron tune (top) and chromaticity (bottom) values as a function of energy calculated using the effective hard-edge dipole models.

The lattice and beam parameters at extraction are given in Table 2. Three cases are given: one for the design parameters calculated using the ideal dipole models, one using the effective hard-edge dipoles and one for the effective dipoles after tune and chromaticity correction using the quadrupole triplets in the straight sections and the trim sextupoles in the arcs. The perturbations introduced by the dipoles are found to have negligible impact on extracted beam parameters.

Table 2: Lattice and Beam Parameters at Extraction

Parameter	Design	Effective	Corrected
$[Q_x, Q_y]$	[12.41,5.38]	[12.39,5.31]	[12.41,5.38]
$[\xi_x, \xi_y]$	[0.72,0.79]	[1.12,2.28]	[0.72,0.79]
ϵ_x (nm)	17.31	17.35	17.43
σ_E (%)	0.086	0.086	0.086
σ_L (ps)	38.0	38.0	38.0

As a final check, the dynamic aperture during the ramp including errors and vacuum chamber eddy currents have been calculated for 20 seeds. In all cases, the effective hard-edge dipole models were used for the calculations. Errors were applied using the standard booster error tables, and tunes and chromaticity were corrected to the original design values. Details of the error magnitudes and correction methods can be found in [1]. The vacuum chamber eddy currents driven by the ramping dipole fields were calculated assuming a 1 mm-thick stainless steel vacuum chamber and 5 Hz offset sine-wave ramping waveform. The resulting change in chromaticity was corrected using the trim sextupoles using the same methods as outlined in [7]. Results are shown in Fig. 6.

Despite the fact the tune shifts with amplitude and energy change significantly when using the effective dipole model compared to the original ideal dipole description, the final dynamic apertures are found to remain comfortably above the physical apertures. The momentum acceptance also remains larger than the ±1.5% provided by the RF bucket.

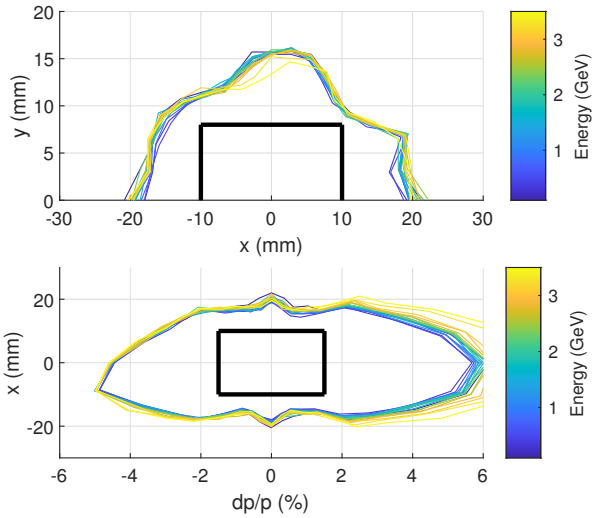

Figure 6: Average on (top) and off (bottom) momentum dynamic apertures over 20 seeds as a function of beam energy.

CONCLUSIONS AND ACKNOWLEDGEMENTS

In this paper we have presented a method for modelling the realistic dipole fields in an efficient and accurate way. Using the effective dipole models, tracking times are substantially reduced to the point whereby they can be used to study multiple errors seeds and long-term particle stability.

For the Diamond-II replacement booster, calculations using the effective dipole models highlighted a significant change in linear optics from the ideal lattice which had to be corrected for in the magnet design stage. Even after these corrections were implemented, tune-shifts with amplitude and energy were found to vary from those predicted using the original ideal dipole models. Despite this, the final ring performance is found to meet the requirements.

Finally, the authors would like to thank J. Kallestrup for initial contributions to this work.

ISBN: 978-3-95450-231-8 ISSN: 2673-5490 doi: 10.18429/JACoW-IPAC2023-WEPL018

REFERENCES

[1] R.P. Walker *et al.*, "Diamond-II Technical Design Report", Aug. 2022. https://www.diamond.ac.uk/Diamond-II.html

[2] I.P.S. Martin *et al.*, "Progress with the Booster Design for the Diamond-II Upgrade", in *Proc. 12th Int. Particle Accelerator Conf. (IPAC'21)*, Campinas, Brazil, May 2021. doi:10.18429/JACoW-IPAC2021-MOPAB071

[3] I.P.S. Martin *et al.*, "Beam Dynamics Studies for the Diamond-II Injector", in *Proc. 13th Int. Particle Accelerator Conf. (IPAC'22)*, Bangkok, Thailand, Jun. 2022. doi:10.18429/JACoW-IPAC2022-THPOPT049

[4] https://www.3ds.com/products-services/simulia/products/opera/

[5] B. Nash *et al.*, "New Functionality for Beam Dynamics in Accelerator Toolbox (AT)", in *Proc. 6th Int. Particle Accelerator Conf. (IPAC'15)*, Richmond, Virginia, USA, May 2015. doi:10.18429/JACoW-IPAC2015-MOPWA014

[6] D. Einfeld *et al.*, "Modelling of Gradient Bending Magnets for the Beam Dynamics Studies at ALBA", in *Proc. 22nd Particle Accelerator Conf. (PAC'07)*, Albuquerque, New Mexico, USA, Jun. 2007, paper TUPMN068, pp. 1076-1078.

[7] M. Munoz and W. Joho, "Eddy Current Effects in the SLS Booster", SLS-TME-TA-1998-0010, Oct. 1998.